Collective ferromagnetism in two-component Fermi-degenerate gas trapped in a finite potential

T. Sogo and H. Yabu
Department of Physics, Tokyo Metropolitan University, 1-1 Minami-Ohsawa, Hachioji, Tokyo 192-0397, Japan
(Received 30 May 2002; published 21 October 2002)

Spin asymmetry of ground states is studied in trapped spin-degenerate (two-component) gases of fermionic atoms with repulsive interaction between different components; and, for a large particle number, the asymmetric (collective ferromagnetic) states are shown to be stable because it can be energetically favorable to increase the Fermi energy of one component rather than increase the interaction energy between up-down components. We formulate the Thomas-Fermi equations and give algebraic methods to solve them. From the Thomas-Fermi solutions, we find three kinds of ground states in the finite system: (1) paramagnetic (spin-symmetric), (2) ferromagnetic (equilibrium), and (3) ferromagnetic (nonequilibrium) states. We present the density profiles and the critical atom numbers for these states obtained analytically, and, in ferromagnetic states, the spin asymmetries are shown to occur in the central region of the trapped gas, and increase with increasing particle number. Based on the obtained results, we discuss the experimental conditions and current difficulties in realizing the ferromagnetic states of the trapped atom gas, which should be overcome.

DOI: 10.1103/PhysRevA.66.043611 PACS number(s): 03.75.Fi, 05.30.Fk

I. INTRODUCTION

Recent developments of laser trapping and cooling of atomic gases, which realized the Bose-Einstein condensates (BEC) for alkali-metal atoms [1], have opened up new interest in condensed atomic gases with multiple components: multicomponent BEC [2,3], Fermi-degenerate (FD) gas [4–6], and also Bose-Fermi mixed gas in trapped potentials [7–10].

One of the interesting physical aspects of such systems is the phase structure in the ground states. In general, multiple-component systems show a variety of phase structures and phase transitions between them. A typical example is seen in superfluid ^{3}He (a system with 2×2 components of orbital and spin angular momenta), where more than two condensed phases resulting from different combinations of condensed components exist [11].

In the condensed system of trapped atomic gases with multiple components, several studies have been done about new phases and phase transitions: the BCS states in attractive two-component Fermi gas [12,13], a transition to the superfluid states in the crossover region between the BCS and BEC theories [14–16], phase separations of different components in the BEC [17–19], Fermi gas [20–22] and Bose-Fermi mixed system [23,24].

In this paper, we discuss the trapped Fermi-degenerate atomic gas with two components: $m=\pm 1/2$ (magnetic quantum number) states of spin-1/2 atoms, or two of the hyperfine states of fermionic atoms with larger total spin ($F>1/2$). Thus, we refer to these components as spin degrees of freedom (up and down components, or up and down atoms) in this paper.

When the interaction between different spin components is weak, the stable ground state of the system has a symmetric state in spin-component distributions at $T=0$ where equal numbers of up and down atoms make similar Fermi-degenerate distributions so that the total spin of the whole system vanishes (paramagnetic state). However, for sufficiently strong interactions between components, an asymmetric state with unequal numbers of up and down atoms can be stable because it can be energetically favorable to increase the Fermi energy of one component rather than increasing the interaction energy between up and down components. (The interaction energy between up-up and down-down components can be neglected due to the Pauli blocking effects.) We call it ''collective ferromagnetic state'' of the two-component Fermi gas.

As the terms ''paramagnetic'' and ''ferromagnetic'' suggest, this theory is related to a mechanism of the metallic magnetism, originally proposed by Bloch and developed by White and Geballe [25], where Fermi particles are the electrons in conductive bands. It should be noted that, in the theory of metallic magnetism, the Hartree-Fock exchange energy plays the role of $E_{\rm int}$. Studies of collective ferromagnetic states of atom gas are also interesting as experimental testing grounds for theoretical ideas in magnetism. Recently, such ferromagnetism aroused new interests in neutron-star physics, as a mechanism of the magnetar (neutron stars with strong magnetic fields) [26].

In the uniform system, such ferromagnetic states have been discussed for the atom gas of ^{6}Li in relation to the stability of the BCS states [12]. The ferromagnetic states have also been discussed on the trapped BEC where the interactions between different spin components are the origin of the asymmetry [27]. In this paper, we study the ferromagnetic states in the trapped and finite fermion system.

In the following section, we formulate a set of equations for the two-component Fermi gas at $T=0$ and the stability condition of its solutions in the Thomas-Fermi (TF) approximations. In Sec. III, solutions of the TF equations are analyzed algebraically, and a critical condition for the collective ferromagnetic states is obtained. In Sec. IV, we show the density distributions of the two-component Fermi gas and discuss paramagnetic-ferromagnetic transitions therein. In Sec. V, we summarize the results and discuss the experimental conditions to obtain the ferromagnetic states.

II. THOMAS-FERMI EQUATIONS FOR THE TWO-COMPONENT FERMI GAS

We consider a $T=0$ system of two-component Fermi gas trapped in an isotropic harmonic-oscillator potential; densities of spin-up and spin-down components are denoted by $\rho_1(r)$ and $\rho_2(r)$. To describe the ground-state behaviors of the system, we use the Thomas-Fermi approximation [12,28], where the total energy of the system is a functional of the densities:

$$E=\int d^3r\left[\sum_{\sigma=1,2}\left\{\frac{\hbar^2}{2m}\frac{3}{5}(6\pi^2)^{2/3}\rho_\sigma^{5/3}+\frac{1}{2}m\omega^2r^2\rho_\sigma\right\}+g\rho_1\rho_2\right]. \tag{1}$$

The m and ω in Eq. (1) are the fermion mass and the oscillator frequency of the trapping potential. The last term in Eq. (1) corresponds to the interaction energy between different components of fermion, and the strength of the coupling constant is given by $g=4\pi\hbar^2a/m$ where a is the s-wave scattering length. The interactions between the same components are neglected; the elastic s-wave scattering is absent because of the Pauli blocking effects and the p-wave scattering is suppressed below $\sim 100\ \mu$K. In the present paper, we discuss a system of repulsive interaction, so that the parameter g should be positive ($g>0$).

As we show later, the collective ferromagnetic states of the two-component Fermi gas show up in the case of large particle number (10^6–10^{13}), which validates the use of the Thomas-Fermi approximation. Also the validity of the approximation can be estimated from the smoothness of the mean-field potential: $V_{\rm eff}=\frac{1}{2}m\omega^2r^2+g\rho_{1,2}$. As a parameter that represents its smoothness, we can take a local de Broglie wavelength $\lambda(r)=\hbar/p(r)$, where $p(r)$ is a TF local momentum defined by $p(r)=\sqrt{2m(\epsilon_F-V_{\rm eff})}$ (ϵ_F: Fermi energy). As presented in Ref. [29], a validity condition with $\lambda(r)$ is given by $f(r)\equiv|d\lambda/dr|\ll 1$. Evaluating $f(r)$ with the parameters given in the preceding section (for ^{40}K), we obtain $f(r)\lesssim 10^{-3}$ except the classical turning points. It also supports the validity of the TF approximations in the present case.

To simplify Eq. (1), we introduce the scaled dimensionless variables,

$$n_\sigma=\frac{128}{9\pi}\rho_\sigma a^3,\quad x=\frac{4}{3\pi}\frac{ar}{\xi^2},\quad \tilde{E}=\frac{2^{18}}{3^7\pi^6}\left(\frac{a}{\xi}\right)^8\frac{E}{\hbar\omega}, \tag{2}$$

where $\xi=\sqrt{\hbar/m\omega}$ is the oscillator length. Using these variables, Eq. (1) becomes

$$\tilde{E}=\int d^3x\left[\sum_{\sigma=1,2}\left(\frac{3}{5}n_\sigma^{5/3}+x^2n_\sigma\right)+n_1n_2\right]. \tag{3}$$

The Thomas-Fermi equations for the densities $n_{1,2}$ are derived from the variations of the total Energy $\tilde{E}$ on $n_{1,2}$ with a constraint on the total particle number $\tilde{N}$: $\delta/\delta n_\sigma(\tilde{E}-\lambda\tilde{N})=0$, where $\tilde{N}$ is the scaled total particle number defined by

$$\tilde{N}=\tilde{N}_1+\tilde{N}_2=\sum_\sigma\int d^3x n_\sigma=\frac{2^{13}}{3^5\pi^4}\left(\frac{a}{\xi}\right)^6N\sim 0.346\left(\frac{a}{\xi}\right)^6N. \tag{4}$$

The Lagrange multiplier λ in the variational equation is for the fermion-number constraint, and is related to the scaled chemical potential $\tilde{\mu}$ through the relation $\tilde{\mu}N=\lambda\tilde{N}$; using Eq. (4), we obtain

$$\tilde{\mu}\sim 0.346\left(\frac{a}{\xi}\right)^6\lambda. \tag{5}$$

It should be noted that, in Eq. (3), parameters (m,ω,g) have been scaled out and no parameters are included except λ. The Lagrange multiplier λ is determined by the total fermion number $\tilde{N}$, so that $\tilde{N}$ is the only parameter that determines the ground-state properties of the system.

Using Eqs. (3) and (4) for the variational equation, we obtain the TF equations

$$n_1^{2/3}+n_2=\lambda-x^2\equiv M(x),\quad n_2^{2/3}+n_1=M(x). \tag{6}$$

The stability condition for solutions of Eq. (6) can be derived from the second-order variations of the energy functional:

$$\begin{vmatrix}\dfrac{\delta^2\tilde{E}}{\delta n_1^2} & \dfrac{\delta^2\tilde{E}}{\delta n_1\delta n_2}\\ \dfrac{\delta^2\tilde{E}}{\delta n_2\delta n_1} & \dfrac{\delta^2\tilde{E}}{\delta n_2^2}\end{vmatrix}\geqslant 0. \tag{7}$$

Using Eq. (3), we obtain the stability condition for the present case:

$$n_1n_2\leqslant\left(\frac{2}{3}\right)^6. \tag{8}$$

III. SOLUTIONS OF THOMAS-FERMI EQUATIONS

In this section, we show solutions of coupled TF equations (6) in an algebraic form and discuss their stability based on the stability condition (8).

Let us introduce variables s and t as $n_1=s^3$ and $n_2=t^3$, then Eq. (6) becomes

$$s^3+t^2=M,\quad t^3+s^2=M. \tag{9}$$

Taking sum and difference of them, we obtain two equations equivalent to Eq. (9):

$$s^3+t^3+s^2+t^2=2M,\quad s^3-t^3-(s^2-t^2)=(s-t)\times(s^2+st+t^2-s-t)=0. \tag{10}$$

The factorized form of the second equation gives two alternatives: (1) $s=t$ or (2) $s^2+st+t^2-s-t=0$.

In case (1), $s=t$, the first equation in Eq. (10) becomes $s^3+s^2=M$, which can be solved algebraically with the Caldano formula. It includes only one positive root when $M\geqslant 0$:

$$s=\frac{f(M)}{6}+\frac{2}{3f(M)}-\frac{1}{3},\quad f(M)=[-8+108M+12\sqrt{81M^2-12M}]^{1/3}. \tag{11}$$

For this solution, the stability condition (8) gives $s\leqslant 2/3$, which leads to the constraint for M,

$$M=s^3+s^2\leqslant\left(\frac{2}{3}\right)^2+\left(\frac{2}{3}\right)^3=\frac{20}{27}. \tag{12}$$

Thus, the stable symmetric solutions exist when $0\leqslant M\leqslant 20/27$.

Next, we take case (2): $s^2+st+t^2-s-t=0$. Now, this and the another equation in Eq. (10) are symmetric under the exchange between s and t, so that they can be represented by elementary symmetric polynomials, $A\equiv s+t$ and $B\equiv st$:

$$A^3-A^2-A+M=0,\quad A^2-A-B=0. \tag{13}$$

The first equation has a real positive solution:

$$A=\frac{g(M)}{6}+\frac{8}{3g(M)}+\frac{1}{3},\quad g(M)=[-108M+44+12\sqrt{81M^2-66M-15}]^{1/3}. \tag{14}$$

Substituting it in Eq. (13), we obtain the solution for B,

$$B=\frac{[g(M)]^2}{36}-\frac{g(M)}{18}+\frac{4}{9}-\frac{8}{9g(M)}+\frac{64}{9[g(M)]^2}. \tag{15}$$

The s and t can be recovered as two solutions of the equation: $x^2-Ax+B=0$. These solutions are generally asymmetric ($s\neq t$).

We can check the stability of the asymmetric solutions with Eq. (8), which gives a constraint for B: $B=st=(n_1n_1)^{1/3}\leqslant 4/9$. Then, from the second equation in Eq. (13), we obtain that for A: $1\leqslant A\leqslant 4/3$. Differentiating the first equation in Eq. (13) by A, we find that M is a monotonically decreasing function of A within the interval $1\leqslant A\leqslant 4/3$. Combining these results, we obtain the stability range of M for the asymmetric solutions: $20/27<M\leqslant 1$.

In summary, the stable solutions of Eq. (10) are

$$0\leqslant M\leqslant\frac{20}{27}\ \text{(symmetric)}, \tag{16a}$$

$$\frac{20}{27}<M\leqslant 1\ \ \text{(asymmetric)}, \tag{16b}$$

$$1<M\ \ \text{(no stable solutions)}. \tag{16c}$$

In the case where $1<M$, Eq. (10) has no stable solution. In the TF variational equation $\delta/\delta n_\sigma(\tilde{E}-\lambda\tilde{N})=0$, we assumed the chemical equilibrium between fermion 1 and 2, and put their chemical potentials (Lagrange multipliers) equal: $\lambda=\lambda_1=\lambda_2$. Accordingly, if $1<M$, we should say that the system has no stable solutions in ''equilibrium.'' Thus, for $1<M$, we should take the nonequilibrium states where all fermions occupy one component (complete asymmetry). If we assume $s=0$, t is obtained by solving the equation

$$t^2=M. \tag{17}$$

IV. DENSITY PROFILES OF THE TWO-COMPONENT FERMI GAS

Using the results of the preceding section, we can calculate the density profiles of the two-component Fermi gas for any value of λ. Corresponding to the classification by $M=\lambda-x^2$ in Eq. (16), we should divide λ into three regions:

$$\text{(i)}\quad 0\leqslant\lambda\leqslant\frac{20}{27},\quad \text{(ii)}\quad \frac{20}{27}<\lambda\leqslant 1,\quad \text{(iii)}\quad 1<\lambda, \tag{18}$$

and discuss qualitative profiles of the density distributions $n_{1,2}$.

(i) *Paramagnetic ground states.* In these cases, $M(x)$ satisfies $M(x)=\lambda-x^2\leqslant 20/27$ for any value of x. Thus, from Eq. (16), the density distributions are composed of the symmetric solution (11) in all spatial regions. Consequently, the ground states are paramagnetic in regions (i): $n_1(x)=n_2(x)$. In Fig. 1(a), the density profiles are shown when $\lambda=1/2$. They decrease monotonically with the scaled radial distance x, and vanish at the TF cutoff: $x_{\mathrm{TF}}\equiv\sqrt{\lambda}=1/\sqrt{2}$ in this case. These states occur in the case of small fermion number.

(ii) *Ferromagnetic ground states in equilibrium.* In these cases, we obtain $M(x)\leqslant 20/27$ in the outside region ($x\geqslant\sqrt{\lambda-20/27}$), but $20/27<M(x)\leqslant 1$ in the inside region ($x<\sqrt{\lambda-20/27}$). Correspondingly, the density distributions become symmetric in the outside region and asymmetric in the inside region, so that the ground states become ferromagnetic in region (ii). Because the condition $M(x)\leqslant 1$ is satisfied, solutions are in equilibrium in all spatial regions, and densities are partially asymmetric in the inside region. In Fig. 1(b), the density profiles are shown when $\lambda=4/5$ for n_1 (solid line) and n_2 (dotted line). The border between symmetric and asymmetric regions is given by $x_{\mathrm{AS}}\equiv\sqrt{\lambda-20/27}=\sqrt{8/135}$ in this case. In the outside (symmetric) region, both the lines overlap and vanish at $x_{\mathrm{TF}}=2/\sqrt{5}$.

(iii) *Ferromagnetic ground states in nonequilibrium.* In these cases, density profiles are also asymmetric in the inside region ($x<x_{\mathrm{AS}}$) as in the above region. However, in the most inside region ($x<\sqrt{\lambda-1}$), $M(x)>1$ is satisfied and, according to (16c) the density profiles become nonequilibrium and are given by complete asymmetric solutions in Eq. (17). In Fig. 1(c), we show the density profiles when $\lambda=3/2$ for n_1 (solid line) and n_2 (dotted line). In the most inside region ($x<x_{\mathrm{EQ}}=\sqrt{\lambda-1}=1/\sqrt{2}$), the density profiles are com-

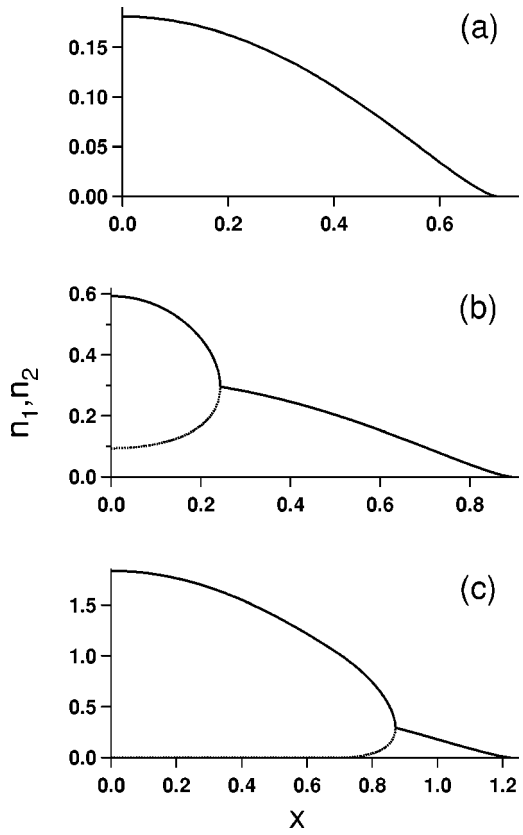

FIG. 1. Density profiles of fermions, n_1 (solid line) and n_2 (dotted line) for (a) $\lambda=0.5$, (b) 0.8, and (c) 1.5. The scaled densities $n_{1,2}$ and the scaled radial distance x are dimensionless and defined by Eq. (2). λ is a (dimensionless) Lagrange multiplier. (a)–(c) correspond to a paramagnetic state (i), a ferromagnetic state in equilibrium (ii), and a ferromagnetic state in nonequilibrium (iii), respectively. The scaled fermion numbers $\tilde{N}_{1,2}$ are $\tilde{N}_1=\tilde{N}_2=0.089$ for (a), $(\tilde{N}_1,\tilde{N}_2)=(0.33,0.31)$ for (b), and $(3.50,0.68)$ for (c).

pletely asymmetric ($n_2=0$), and, in $x_{\rm EQ}\leqslant x<x_{\rm AS}=\sqrt{41/54}$, they are partially asymmetric. In the outside (symmetric) region ($x>x_{\rm AS}$), two lines overlap and vanish at $x=x_{\rm TF}=\sqrt{3/2}$. Thus, the ground states are ferromagnetic and in nonequilibrium in region (iii), which corresponds to the case of large fermion number.

In Fig. 2, we show the dependence of λ on the fermion

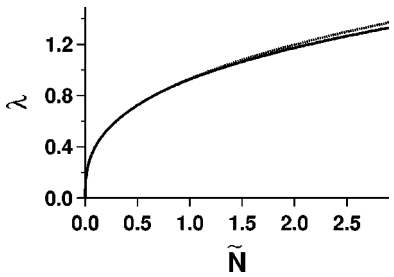

FIG. 2. Lagrange multiplier λ against the scaled fermion number $\tilde{N}$. The solid and dotted lines are for the ground and paramagnetic states. λ is introduced as a Lagrange multiplier for fermion-number constraint, and $\tilde{N}$ is defined by Eq. (4). Both quantities are dimensionless.

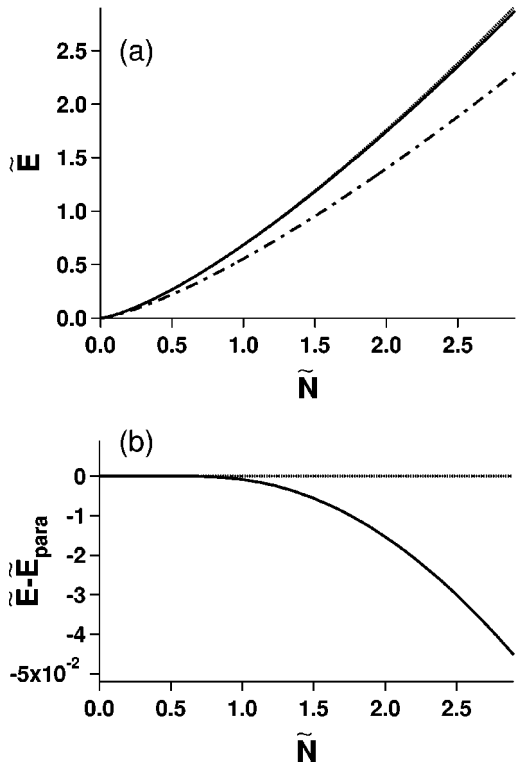

FIG. 3. (a) The scaled total energy $\tilde{E}$ against the scaled total fermion number $\tilde{N}=\tilde{N}_1+\tilde{N}_2$: the solid line is for the ground states and the dotted one is for the paramagnetic states. The dash-dotted line is for the total energy of the noninteracting fermionic system, $\tilde{E}_{\rm non}=\frac{3}{16}\pi^2[(4/\pi^2)\tilde{N}]^{4/3}$. (b) The energy differences from that of the paramagnetic states, $\tilde{E}-\tilde{E}_{\rm para}$. The solid and dotted lines are for the ground and paramagnetic states.

number $\tilde{N}$, which is calculated by Eq. (4) using the fermion densities $n_{1,2}(x)$ obtained above; for the ground states (solid line) and the paramagnetic states (dotted line). From the above discussion, for $\lambda\leqslant 20/27$, the ground states are paramagnetic, so that both the lines overlap. As can be seen in this figure, the critical value $\lambda=20/27$ corresponds to $\tilde{N}_C=0.53$, which is the critical fermion number for the transition between paramagnetic and ferromagnetic states.

In Fig. 3(a), variations of scaled total energies $\tilde{E}$ are shown against $\tilde{N}$, for the ground (solid line) and paramagnetic (dotted) states. $\tilde{E}$ can be obtained by Eq. (3) as a function of λ using the fermion densities $n_{1,2}(x)$; combined with the $\tilde{N}$ dependence of λ (shown in Fig. 2), we can obtain its $\tilde{N}$ dependence. In $\tilde{N}\leqslant\tilde{N}_C=0.53$, both lines overlap completely because the ground states become paramagnetic. In Fig. 3(b), we plot the energy difference between the ground and paramagnetic states. In this figure, we can find that, if $\tilde{N}>\tilde{N}_C$, the ground-state energy (solid line) shifts lower than that of the paramagnetic states (dotted line); it shows that the ferromagnetic ground states become more stable in this region.

As can be seen in Fig. 3(a) when $\tilde{N}>0.53$, the energy difference between the ferromagnetic and paramagnetic states $|\tilde{E}-\tilde{E}_{\rm para}|$ is very small in comparison with the total energy $\tilde{E}$: e.g., $|\tilde{E}-\tilde{E}_{\rm para}|/\tilde{E}\sim 0.01$ at $\tilde{N}=2.0$. A large part of

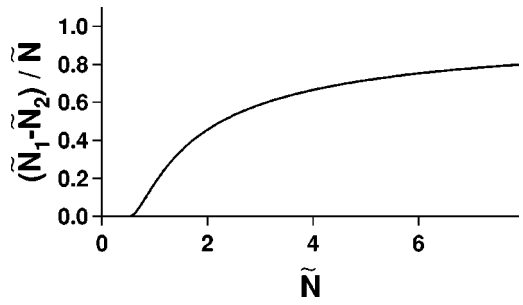

FIG. 4. Variation of the fermion-number asymmetry $(\tilde{N}_1-\tilde{N}_2)/\tilde{N}$ against the scaled total fermion number $\tilde{N}$. The solid and dotted lines are for the ground and paramagnetic states, respectively.

$\tilde{E}$ consists of the stacked kinetic energy due to the Fermi degeneracy of fermions. Roughly speaking, its size can be estimated from the total energy of the noninteracting Fermi gas $(g=0)$ trapped in the same harmonic-oscillator potential; $\tilde{E}_{\rm non}=\frac{3}{16}\pi^2[(4/\pi^2)\tilde{N}]^{4/3}$, which increases rapidly with increasing $\tilde{N}$. The $\tilde{E}_{\rm non}$ is plotted also in Fig. 3(a) (dot-dashed line), the amounts of which are almost $\sim 75\%$ of $\tilde{E}$.

However, to evaluate the scale of the energy difference, we should compare it with an one-particle excitation energy at the Fermi surface, which can be estimated from the scaled chemical potential $\tilde{\mu}$ defined in Eq. (5). In the case of ^{40}K with the harmonic-oscillator frequency $\omega=1000$ Hz (for other parameters, see the following section), Eq. (5) becomes $\tilde{\mu}\sim 10^{-13}\lambda$. When $\tilde{N}\sim 2$ ($\lambda\sim 1$ from Fig. 2), the ratio $\Delta\tilde{E}/\tilde{\mu}$ becomes 10^{13}. Thus, we should say that the energy difference between the ferromagnetic and paramagnetic states is fairly large.

In Fig. 4, we show the fermion-number asymmetry $(\tilde{N}_1-\widetilde{N_2})/\tilde{N}=(N_1-N_2)/(N_1+N_2)$ against the total fermion number $\tilde{N}$.

V. SUMMARY AND DISCUSSIONS

We discussed the possibility of transition to ferromagnetic states in the two-component Fermi gas using the Thomas-Fermi approximation from theoretical points of view. Based on the results that we obtained, let us discuss experimental conditions and also difficulties to observe ferromagnetic ground states in the trapped atomic gas. We hope that these difficulties are overcome in future developments in experimental technics.

As shown in the preceding section, the ferromagnetic ground states become stable when $\tilde{N}\gtrsim 0.53$; using Eq. (4), the unscaled critical number N_C becomes

$$N_C\sim\frac{0.53}{0.346}\left(\frac{\xi}{a}\right)^6=1.5\left(\frac{\xi}{a}\right)^6. \tag{19}$$

As an example, we take the ^{40}K atoms (mass $m=0.649\times 10^{-25}$ kg) trapped in the harmonic oscillator potential with $\omega=1000$ Hz. For the scattering length, we take the value $a=169a_B$ (a_B: Bohr radius) given in Ref. [30]. Using these parameters, we obtain $N_C\sim 10^{13}$. In recent experiments, the trapped Fermi-degenerate gas has been observed up to $\sim 10^6$ atoms, so that a larger trapping potential is necessary for the realization of the ferromagnetic ground state than the currently used one. In addition, because of the high central density ($\sim 10^{17}$ cm^{-3}) for $\sim 10^{13}$ atoms, the inelastic/multiple-body scattering processes in them become important, which might destroy the trapped atoms before they reach the required density.

There can be several possibilities for the reduction of N_C. For example, if the scattering length can be increased by the Feshbach resonance for ^{40}K, which has been observed experimentally [6], the value of N_C decreases and the ferromagnetic ground states can be obtained in small fermion number: simple estimation gives, $a=820a_B$ for $N_C\sim 10^9$ and $a=2600a_B$ for $N_C\sim 10^6$. However, in current experiments, the tuning into Feshbach resonances is done by applying the magnetic field, which should lead to the energy difference between the up and down states and makes the ferromagnetic transition into a crossover in the spin asymmetry. Tuning Feshbach resonances by nonmagnetic external forces (e.g., electric fields) is preferred for the present purpose.

The use of heavier elements, e.g., Sr or Yb, is also effective for the ferromagnetic states. We hope that the combination of these methods may lead to the experimental achievements.

We also comment on the process to observe the ferromagnetic states. There exist two possibilities.

(a) The experiment starts with the magnetic field in some direction that results in the spin asymmetry (e.g., $N_1>N_2$). Then, the magnetic field is switched off adiabatically in the cooling process. When the number of the remaining atoms is large enough, it shows the ferromagnetic states.

(b) The experiment starts with the symmetric trap ($N_1=N_2$), and, after some relaxation time elapses, the atoms release their spin angular momenta and become the ferromagnetic state.

Case (a) is similar to a standard process for observing the phase transition in the ferromagnetic materials. In case (b), the spin-relaxation time is considered to be of the same order as that of clusterization, so that it might be difficult to observe the ferromagnetic transition within the lifetime of the atomic gas.

Finally, we comment on the spatially phase-separated states in the trapped fermionic gas in the case of the large particle number and interaction strength [20–22]. They correspond to the phase separation in the uniform system (two-phase coexistent region), discussed in Ref. [12]. The naive TF calculations give smaller energy for the ferromagnetic states, but the energy difference is very small. The competition (or coexistence) of these states should be an interesting problem for future studies.

ACKNOWLEDGMENTS

We are very grateful to T. Maruyama, T. Suzuki, and T. Miyakawa for fruitful discussions. Special thanks are also due to T. Tatsumi for introducing to us the physics of collective ferromagnetism.

[1] For a review, see W. Ketterle, D. S. Durfee, and D. M. Stamper-Kurn, in *Bose-Einstein Condensation in Atomic Gases*, Proceedings of International School of Physics ''Enrico Fermi,'' edited by M. Inguscio, S. Stringari, and C. Wieman (IOS Press, Amsterdam, 1999).
[2] J. Stenger, S. Inouye, D.M. Stamper-Kurn, H.-J. Miesner, A.P. Chikkatur, and W. Ketterle, Nature (London) **396**, 345 (1998).
[3] M.D. Barrett, J.A. Sauer, and M.S. Chapman, Phys. Rev. Lett. **87**, 010404 (2001).
[4] B. DeMarco and D.S. Jin, Science **285**, 1703 (1999).
[5] S.R. Granade, M.E. Gehm, K.M. O'Hara, and J.E. Thomas, Phys. Rev. Lett. **88**, 120405 (2002).
[6] T. Loftus, C.A. Regal, T. Ticknor, J.L. Bohn, and D.S. Jin, Phys. Rev. Lett. **88**, 173201 (2002).
[7] A.G. Truscott, K.E. Strecker, W.L. McAlexander, G.B. Partridge, and R.G. Hulet, Science **291**, 2570 (2001).
[8] F. Schreck, L. Khaykovich, K.L. Corwin, G. Ferrari, T. Bourdel, J. Cubizolles, and C. Salomon, Phys. Rev. Lett. **87**, 080403 (2001).
[9] J. Goldwin, S.B. Papp, B. DeMarco, and D.S. Jin, Phys. Rev. A **65**, 021402 (2002).
[10] Z. Hadzibabic, C.A. Stan, K. Dieckmann, S. Gupta, M.W. Zwierlein, A. Gorlitz, and W. Ketterle, Phys. Rev. Lett. **88**, 160401 (2002).
[11] G.E. Volovik, *Exotic Properties of Superfluid* ^3He (World Scientific, Singapore, 1992).
[12] M. Houbiers, R. Ferwerda, H.T.C. Stoof, W.I. McAlexander, C.A. Sackett, and R.G. Hulet, Phys. Rev. A **56**, 4864 (1997).
[13] M.A. Baranov and D.S. Petrov, Phys. Rev. A **58**, R801 (1998).
[14] M. Holland, S.J.J.M.F. Kokkelmans, M.L. Chiofalo, and R. Walser, Phys. Rev. Lett. **87**, 120406 (2001).
[15] E. Timmermans, K. Furuya, P.W. Milonni, and A.K. Kerman, Phys. Lett. A **285**, 228 (2001).
[16] Y. Ohashi and A. Griffin, Phys. Rev. Lett. **89**, 130402 (2002).
[17] P. Ohberg and S. Stenholm, Phys. Rev. A **57**, 1272 (1998).
[18] H. Pu and N.P. Bigelow, Phys. Rev. Lett. **80**, 1130 (1998).
[19] D. Gordon and C.M. Savage, Phys. Rev. A **58**, 1440 (1998).
[20] M. Amoruso, I. Meccoli, A. Minguzzi, and M.P. Tosi, Eur. Phys. J. D **8**, 361 (2000); Z. Akdeniz, P. Vignolo, A. Minguzzi, and M.P. Tosi, J. Phys. B: At. Mol. Opt. Phys. **35**, L105 (2002).
[21] L. Salasnich, B. Pozzi, A. Parola, and L. Reatto, J. Phys. B: At. Mol. Opt. Phys. **33**, 3943 (2000).
[22] R. Roth and H. Feldmeier, J. Phys. B: At. Mol. Opt. Phys. **34**, 4629 (2001).
[23] K. Mølmer, Phys. Rev. Lett. **80**, 1804 (1998).
[24] N. Nygaard and K. Mølmer, Phys. Rev. A **59**, 2974 (1999).
[25] R.M. White and T.H. Geballe, *Long Range Order in Solids*, Solid State Physics Vol. 15 (Academic Press, New York, 1979).
[26] T. Tatsumi, Phys. Lett. B **489**, 280 (2000); T. Maruyama and T. Tatsumi, Nucl. Phys. A **693**, 710 (2001).
[27] T.-L. Ho, Phys. Rev. Lett. **81**, 742 (1998).
[28] P. Ring and P. Schuck, *The Nuclear Many-Body Problem* (Springer-Verlag, New York, 1980).
[29] L.D. Landau and E.M. Lifschitz, *Quantum Mechanics Non-Relativistic Theory*, Course in Theoretical Physics Vol. 6, 3rd ed. (Butterworth-Heinemann, Oxford, 1997).
[30] H. Wang *et al.*, Phys. Rev. A **62**, 052704 (2000).